Infrared Spectra of Perdeuterated Naphthalene, Phenanthrene, Chrysene, and Pyrene

Charles W. Bauschlicher, Jr.,* Stephen R. Langhoff, and Scott A. Sandford

NASA Ames Research Center, Moffett Field, California 94035

Douglas M. Hudgins

Department of Chemistry, Adrian College, Adrian, Michigan 49221

Received: November 8, 1996; In Final Form: January 17, 1997[⊗]

Calculations are carried out using density functional theory (DFT) to determine the harmonic frequencies and intensities of perdeuterated naphthalene, phenanthrene, pyrene, and chrysene. We also report matrix-isolation spectra for these four species. The theoretical and experimental frequencies and relative intensities for the perdeuterated species are in generally good agreement. The effect of perdeuteration is to reduce the sum of the integrated intensities by a factor of about 1.75. This reduction occurs for all vibrational motions, except for the weak low-frequency ring deformation modes. There is also a significant redistribution of the relative intensities between the out-of-plane C−D bands relative to those found for the out-of-plane C−H bands. The theoretical isotopic ratios provide an excellent diagnostic of the degree of C−H(C−D) involvement in the vibrational bands, allowing in most cases a clear distinction of the type of motion.

I. Introduction

Polycyclic aromatic hydrocarbons (PAHs) are thought to be ubiquitous and abundant in interstellar space.[1,2] PAHs of intermediate size are expected to become deuterium enriched in space through the selective loss of hydrogen during photodissociation events.[1,3] This process is temperature independent and is expected to occur for PAHs exposed to UV radiation. For PAHs in the appropriate size range, the number of degrees of internal freedom is sufficiently small that, after the absorption of a UV photon, enough energy can be concentrated in a specific bond to induce bond rupture before radiative relaxation occurs. The most likely bonds to be broken are those between peripheral carbon atoms in the aromatic skeleton and their attached hydrogen atoms. Since the aromatic C−D bond has a zero-point energy that is about 30% lower than that of the aromatic C−H bond, hydrogen loss is favored over deuterium loss. For PAHs exposed to the interstellar radiation field, the rupture rate is expected to be 2.5−3.5 times larger for C−H than for C−D.[1] Once a peripheral H is lost, the resulting molecular site is free to bond with the next molecular species the PAH encounters. In the interstellar medium, this will most likely be another H atom, but will occasionally be a deuterium atom or other atomic or molecular species. In typical interstellar environments, such photodissociation events are expected to happen to small PAHs on the order of once per year.[4] Since the cosmic D/H ratio is $\approx 10^{-5}$, small PAHs would be expected to replace one hydrogen atom with a deuterium atom on time scales on the order of 10^5 years.

Similar enrichments by this process are not expected for the known nonaromatic interstellar molecules because, unlike the PAHs, they are not stable against complete photodestruction. There is currently evidence gathered from the study of meteorites that supports the idea that this process is occurring in interstellar space. The carbonaceous fraction of primitive meteorites and collected samples of interplanetary dust are known to contain a variety of different PAHs.[3,5,6] The carbonaceous fractions of these meteorites and dust grains are also observed to carry extremely large deuterium isotopic enrichments.[7,8] These enrichments have long been accepted as evidence that some or all of these organic fractions have an interstellar origin.[9] Studies of the different molecular components of these carbonaceous fractions have demonstrated that one of the major carriers of deuterium is the PAHs.[10] Furthermore, the distribution of D in the meteoritic organics is qualitatively consistent with the suggested photodissociation process. Photodissociational D enrichment in interstellar PAHs is expected to be most significant for molecules in the range of sizes spanned by naphthalene ($C_{10}H_8$, C/H = 1.25) and hexabenzocoronene ($C_{42}H_{18}$, C/H = 2.33).[3] Deuterium enrichments are not expected in benzene because this aromatic molecule is not stable in the interstellar radiation field. Enrichments in PAHs containing more than about 40 carbon atoms are not expected because they have a sufficiently large number of internal degrees of freedom to absorb UV photons without any subsequent bond rupture occurring. Comparisons of the D/H ratio versus C/H ratio in meteoritic organics show just this sort of distribution.[3,11,12]

To gain some insight into the effect of deuteration on the spectra of PAHs, we report here a joint theoretical and experimental study of four perdeuterated neutral PAHs, namely, naphthalene, phenanthrene, pyrene, and chrysene. Although one would not expect perdeuterated species to exist in interstellar space considering the low D/H ratios, we felt that perdeuteration was the least ambiguous approach of examining the effect of deuteration. We find that the isotopic ratios are very useful for identifying the nature of the vibrational motion for the bands. The scaled theoretical harmonics obtained using density functional methods are in excellent agreement with the fundamentals observed in matrix isolation, as are the relative intensities. A considerable number of weak overtone and combination bands are also observed in the matrix. The theoretical harmonics for both hydrogenated and deuterated pyrene are also in excellent agreement with earlier infrared and Raman spectra obtained in solution and in the solid.[13,14] With a few exceptions the band assignments of the earlier study are shown to be correct.

II. Methods

We follow the approach used in our earlier study[15] of neutral PAHs in that we compute the harmonic frequencies using the

[⊗] Abstract published in *Advance ACS Abstracts,* March 1, 1997.

S1089-5639(96)03740-1 CCC: $14.00

density functional theory (DFT) approach. We use the B3LYP hybrid functional,[16] which includes some rigorous Hartree−Fock exchange as well as a gradient correction for both exchange[17] and correlation.[18] The B3LYP calculations were performed using the Gaussian 92/DFT computer codes[19] on the Computational Chemistry IBM RISC System/6000 computers.

We have used the 4-31G basis set[20] throughout. Calibration calculations,[21] which have been carried out for the fully hydrogenated systems, show that a single scale factor of 0.958 brings the B3LYP harmonic frequencies computed using the 4-31G basis set into excellent agreement with the experimental fundamentals; for example, in naphthalene the average absolute error is 4.4 cm^{-1} and the maximum error is 12.4 cm^{-1}. Using the 6-31G* basis set increases the average and maximum error to 11.2 and 36.3 cm^{-1}, respectively. For the 6-31G* basis set, scaling the C−H stretch separately (i.e. using two scale factors) yields average and maximum errors for the non-C−H stretches of 6.2 and 15.1 cm^{-1} and 0.4 and 2.5 cm^{-1} for the C−H stretches. Thus using two scale factors in conjunction with the 6-31G* basis set still produces a larger error than the 4-31G basis set with one scale factor. For large basis sets, such as 6-311G(2d,2p), the two scale factor results are superior to those obtained with the 4-31G basis set and one scale factor; however, such sets are impractical for the largest systems.

While scaling the 4-31G harmonics yields very reliable frequencies, the calibration calculations[21] also show that the computed B3LYP/4-31G intensities are accurate except for C−H stretch. For CH and naphthalene increasing the basis set reduces the C−H stretching intensities.[21] For CH very accurate calculations show that the intensity of the fundamental is very similar to the large basis set B3LYP result within the double-harmonic approximation, while the B3LYP/4-31G result is about a factor of 2 larger. For naphthalene the difference between the B3LYP results using the 4-31G and largest set is somewhat less than a factor of 2. Thus the B3LYP/4-31G C−H stretching intensities are expected to be about a factor of 2 larger than the experimental gas-phase results. Since the gas-phase results[22] tend to lie between the theoretical and matrix isolation values, it is possible that the matrix may slightly reduce the C−H stretching intensity. We should note that for two closely spaced bands of the same symmetry the relative intensity of the bands is somewhat sensitive to the level of theory, and thus the sum of their intensities is more reliable than the individual values. For naphthalene,[21] excluding the C−H stretching intensities, the average absolute difference between the B3LYP/4-31G and B3LYP/6-31++G** intensities is smaller than the corresponding difference between the B3LYP/6-31G* and B3LYP/6-31++G** intensities.

Overall the calculations support the use of the B3LYP/4-31G approach using a uniform scaling factor for the frequencies. The only systematic error is the approximately factor of 2 overestimation of the C−H stretching intensity. In addition this basis set facilitates a comparison with our earlier work[15] for the hydrogenated species and can be used to study larger systems. It should be noted, however, that this approach relies on a cancellation of errors, and while it can be applied with confidence to the PAH molecules since they have similar bonding, it should not be applied to other systems without additional calibration studies.

III. Experimental Section

The matrix-isolation technique was employed to isolate individual perdeuterated polycyclic aromatic hydrocarbon (PAH) molecules in an argon matrix, where their infrared spectra were measured. Argon matrices are known to be suitable for vibrational studies, typically causing small band frequency shifts in the 0−15 cm^{-1} range. The experimental apparatus and methodology have been described in detail previously[23,24] and will be reviewed only briefly here.

Briefly, an infrared transparent window (CsI) is suspended inside an ultrahigh-vacuum chamber ($P \approx 10^{-8}$ mTorr) and cooled by a closed-cycle helium refrigerator. The vacuum chamber is equipped with multiple inlet ports, and the cooler is mounted in such a way that the infrared window can be rotated to face any of these ports without breaking vacuum. Initially, the CsI window is cooled to 10 K and positioned to face a sample deposition inlet. Samples were prepared by co-deposition of a gaseous PAH with a large overabundance of argon to a thickness appropriate for measurement of the PAH's infrared spectrum.

The PAHs used in this investigation were naphthalene-d_8 (Cambridge Isotope Laboratories, 99% purity), phenanthrene-d_{10} (Aldrich, 97% purity), pyrene-d_{10} (Cambridge Isotope Laboratories, 98% purity), and chrysene-d_{12} (Cambridge Isotope Laboratories, 98% purity). All samples were used without further purification. Matheson prepurified argon (99.998% min.) was used in these studies.

Naphthalene-d_8 is sufficiently volatile that it was possible to premix it in a sample bulb with a known amount of argon at room temperature. The data presented here were obtained from an Ar/naphthalene-d_8 mixture of 600/1. Unfortunately, PAHs containing three or more rings do not have sufficient vapor pressure at room temperature to permit their preparation as a gaseous mixture with argon. This necessitates thermal vaporization of a solid sample of the PAH of interest and subsequent co-deposition of the gaseous PAH molecules with larger amounts of argon. To this end, our remaining PAH samples were placed individually in resistively heated Pyrex tubes mounted on the sample chamber. Sample temperatures were monitored using a chromel/alumel type K thermocouple mounted on the exterior of the tube. During PAH volatilization, argon was admitted through an adjacent inlet port in such a way that the two "streams" coalesced and froze together on the surface of the cold window. The argon deposition line was liquid nitrogen trapped to minimize contamination.

Sample quality was found to be optimal for PAH deposition vapor pressures in the range 10−30 mTorr. Higher vapor pressures required higher argon deposition rates, which exceeded the thermal conductivity of the CsI window, thereby warming the matrix and resulting in "annealing", which increased scattering at short wavelengths. Conversely, lower vapor pressures require longer deposition times, which necessarily increased contamination (primarily H_2O) in the matrix. Optimum tube temperatures for the PAHs discussed here were phenanthrene-d_{10}, cooled to 9 °C, pyrene-d_{10}, heated to 65 °C, and chrysene-d_{12}, heated to 100 °C. The optimal argon flow rate was estimated to be between 0.5 and 1.0 mmol/h. On the basis of our argon flow rates and the PAH deposition rates estimated from measured band areas using the theoretical intrinsic band strengths presented later in this paper, we can estimate the Ar/PAH ratios for the phenanthrene-d_{10}, pyrene-d_{10}, and chrysene-d_{12} deposited in this manner. It was found that in all three cases the argon to PAH ratios of our samples were well in excess of 2000. Thus, all four of our perdeuterated PAH samples were well isolated in argon.

After sample deposition was complete, the cold head was rotated to face the beam of an infrared spectrometer so the spectrum could be recorded and ratioed against a "blank" spectrum that was measured prior to sample deposition. The sample chamber was equipped with CsI vacuum windows and suspended in the sample compartment of an FTIR spectrometer (Nicolet Analytical Instruments, Model 740). Mid-infrared

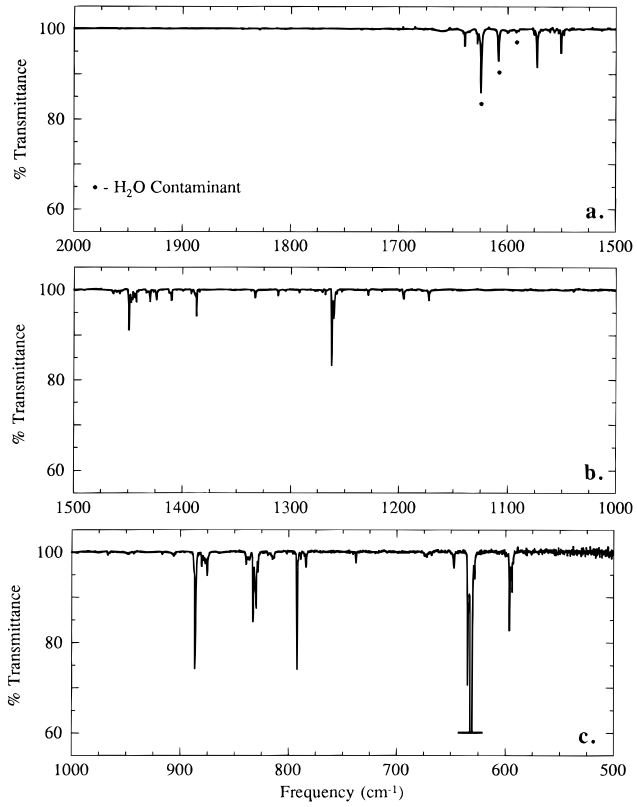

Figure 1. Spectra of matrix-isolated perdeuterated naphthalene-d_8 ($C_{10}D_8$) through the aromatic CC stretching and CD bending regions: (a) 2000−1500 cm^{-1}, (b) 1500−1000 cm^{-1}, and (c) 1000−500 cm^{-1}. The spectra were taken at 10 K, and the argon to naphthalene-d_8 ratio was 600/1. Bands due to contaminant matrix-isolated H_2O are indicated with a dot (•).

spectra (7000−500 cm^{-1}) were collected using an MCT-B detector/KBr beamsplitter combination. All spectra reported here were measured at a resolution of 1 cm^{-1} with a data sampling interval of 0.25 cm^{-1}. Spectra were typically generated through coaddition of 5 blocks of 200 scans, a number that optimized both the signal-to-noise ratio and time requirements of each experiment.

IV. Results and Discussion

Our matrix-isolation spectra of perdeuterated naphthalene ($C_{10}D_8$) are shown in Figures 1 and 2. The theoretical and experimental infrared frequencies and intensities for perdeuterated naphthalene are compared in Table 1. The absolute theoretical intensities are given first with relative values in parentheses. The relative values are given with respect to the strongest out-of-plane bend that lies in the range 630−635 cm^{-1}. The isotopic ratio of the fully hydrogenated to perdeuterated frequencies is computed for the B3LYP results and also reported in the table using our earlier theoretical results[15] for $C_{10}H_8$. Note that while we have included all experimental bands with relative intensity greater than 0.01 in the table, we have not included the weak bands (<0.01) unless they appear to correspond to one of the theoretical bands. To easily compare the theoretical and experimental spectra, we have constructed experimental and theoretical spectra (see Figure 3) using the data in Table 1. We use a full width at half-maximum (fwhm) of 10 cm^{-1}; this is consistent with the broadest bands in experiment and allows an easy presentation of the spectral range from 0 to 2000 cm^{-1} in one figure. A comparison of Figures 1 and 2 with 3 shows that this is a reasonable reproduction of the experimental spectra, excluding the structure in some of the bands. This plot shows the similarity of the theoretical and experimental spectra. It also clearly shows the differences: theory is finding moderately strong bands at frequencies below the range of our spectrometer,

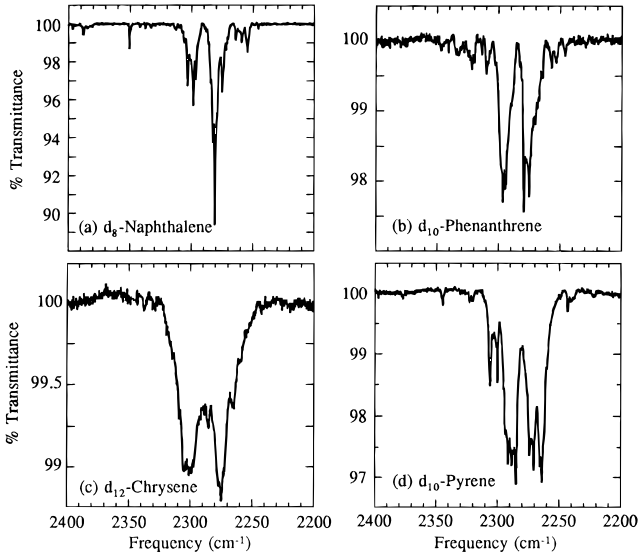

Figure 2. Spectra in the 2400−2200 cm^{-1} C−D stretching region of the matrix-isolated perdeuterated PAHs (a) naphthalene-d_8 ($C_{10}D_8$), (b) phenanthrene-d_{10} ($C_{14}D_{10}$), (c) chrysene-d_{12} ($C_{18}D_{12}$), and (d) pyrene-d_{10} ($C_{16}D_{10}$). All spectra were taken at a temperature of 10 K. The argon to PAH ratio was 600/1 for the naphthalene-d_8 and in excess of 2000 for the other PAHs.

TABLE 1: Comparison of Theoretical and Experimental Infrared Frequencies (cm^{-1}) and Intensities (km/mol) for Perdeuterated Naphthalene

	theory			experiment	
irrep	freq[a]	intensity[b]	ratio[c]	freq	rel int
b_{3u}	158.6	1.86(0.042)	1.084		
b_{1u}	328.6	1.02(0.023)	1.098		
b_{3u}	405.7	20.16(0.451)	1.183		
b_{2u}	605.9	3.38(0.076)	1.043	593.7,596.0	0.092
b_{3u}	631.1	44.70(1.000)	1.249	630.9,634.3	1.000
				647.1	0.013
b_{1u}	739.8	0.14(0.003)	1.078	737.5	<0.01
				783.4,785.0,788.4	0.019
b_{3u}	796.1	6.61(0.148)	1.210	791.6	0.112
b_{2u}	831.7	5.39(0.121)	1.214	829.8,832.5	0.170
b_{2u}	846.8	0.12(0.003)	1.381	836.0,838.0,839.0	0.030
				874.9,876.7,877.9,880.0	0.064
b_{1u}	886.0	6.58(0.147)	1.278	886.0	0.177
				905.7	0.012
b_{1u}	1055.7	0.10(0.002)	1.203	1038.6	<0.01
b_{2u}	1085.6	0.03(0.001)	1.114		
				1172.1	0.022
				1195.2	0.019
b_{1u}	1241.6	3.46(0.077)	1.128	1259.7,1261.6	0.136
b_{2u}	1311.9	0.28(0.006)	1.035	1332.4	0.011
				1386.8 complex	0.047
				1409.6	0.023
				1423.7	0.014
				1429.4	0.020
b_{2u}	1435.1	2.95(0.066)	1.051	1448.8 complex	0.104
				1466.5	0.029
b_{1u}	1543.4	0.79(0.018)	1.032	1550.2	0.048
				1572.3	0.077[d]
				1638.8	0.018
b_{1u}	2244.0	2.26(0.051)	1.356		
b_{2u}	2247.0	1.97(0.044)	1.355		
b_{1u}	2268.3	50.37(1.127)	1.350	2250−2315[e]	1.124
b_{2u}	2282.2	36.44(0.815)	1.348		

[a] The B3LYP/4-31G frequencies are scaled by 0.958. [b] The relative intensities are given in parentheses. [c] The ratio of the hydrogen/deuterium frequencies. [d] The band is overlapped by a band due to small amounts of contaminant H_2O, and therefore the intensity may be less accurate than for the other bands. [e] Main band is at 2280.0 cm^{-1}: see Figure 2.

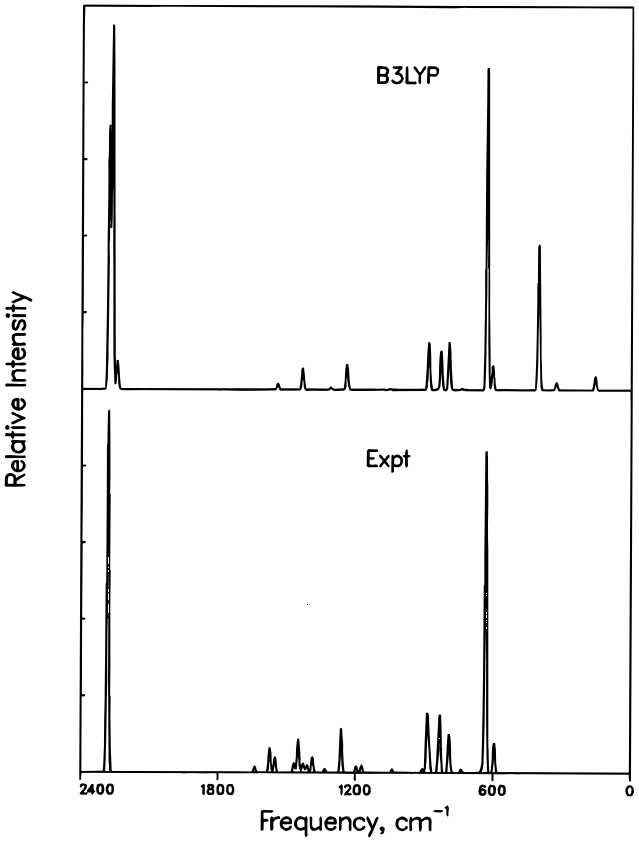

Figure 3. Comparison of synthetic naphthalene-d_8 spectra constructed using the experimental and theoretical data in Table 1. The fwhm is 10 cm^{-1}.

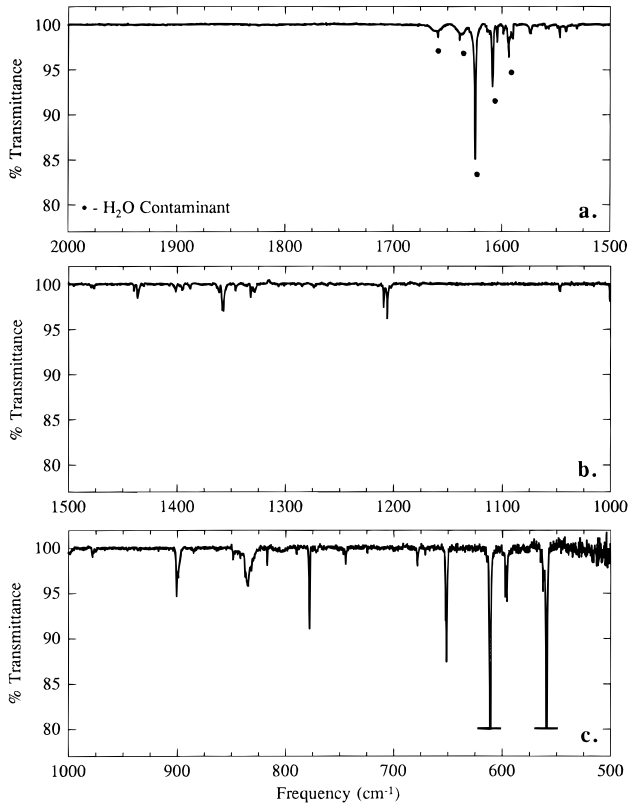

Figure 4. Spectra of matrix-isolated perdeuterated phenanthrene-d_{10} ($C_{14}D_{10}$) through the aromatic CC stretching and CD bending regions: (a) 2000−1500 cm^{-1}, (b) 1500−1000 cm^{-1}, and (c) 1000−500 cm^{-1}. The spectra were taken at 10 K, and the argon to phenanthrene-d_{10} ratio was in excess of 2000/1. Bands due to contaminant matrix-isolated H_2O are indicated with a dot (•).

and many combination and overtone bands are observed in experiment.

The lowest two frequency modes with isotopic ratios between 1.08 and 1.10 are primarily ring deformation modes and are relatively weak. The much stronger band at 405.7 cm^{-1} has a larger component of C−D out-of-plane bend, as evidenced by an isotopic ratio of 1.18. This band lies just outside the range of our spectrometer and is consequently not observed. Although we do not have matrix isolation data for these low-frequency modes, we believe that the shifted theoretical frequencies are accurate based on the good agreement with the far-infrared emission spectra of selected hydrogenated PAHs obtained in the gas phase by Zhang *et al.*[25] The next theoretical band at 605.9 cm^{-1} is again primarily a ring deformation mode, which we correlate with the two closely spaced peaks in the experimental spectrum at 593.7 and 596.0 cm^{-1}, which sum to about the same relative intensity. The band is probably split due to matrix effects. The strongest band in this region lies at 631.1 cm^{-1} (theoretical) and based on the isotopic ratio is clearly due to out-of-plane bending. Theory is in good agreement with the observed spectrum, which has two peaks at 630.9 and 634.3 cm^{-1}. The weak experimental band at 647.1 cm^{-1} cannot be correlated with any of the scaled B3LYP harmonics, and therefore we conclude that it is probably a combination or overtone band instead of a fundamental. The B3LYP calculations predict two nearly equally intense CH out-of-plane bending bands at 796.1 and 831.7 cm^{-1}. Experiment is consistent in finding a moderately strong band at 791.6 cm^{-1} and one in the 829−833 cm^{-1} region. Experimental bands are also observed between 836 and 839 cm^{-1}, which are possibly the weak b_{2u} harmonic at 846.8 cm^{-1}. The bands between 874 and 880 cm^{-1} cannot be correlated with any of the theoretical harmonics and are thus likely due to multiple sites in the matrix or due to combination and overtone bands. Theory and experiment are again consistent in finding a moderately strong peak at 886 cm^{-1}.

The theoretical spectrum in the energy range 1000−1600 cm^{-1} corresponding to in-plane C−D bend and C−C stretching motions is very weak, as it was for hydrogenated naphthalene. Only two moderately weak bands are found in the calculations, namely, a b_{1u} band at 1241.6 cm^{-1} and a b_{2u} band at 1435.1 cm^{-1}. The isotopic ratios show that the former contains more C−D bend involvement than the latter, which is almost pure C−C stretch. Experimentally, many more bands are observed, but overall the spectrum is rather weak in this spectral range. We correlate the b_{1u} harmonic with the bands observed between 1259 and 1262 cm^{-1} and the b_{2u} harmonic with the complex of peaks at 1448.8 cm^{-1}. It is likely that the experimental bands at 1550.2, 1572.3, and 1638.8 cm^{-1} are overtone and combination bands.

The C−D stretches, two each of b_{1u} and b_{2u} symmetry, lie in the spectral range 2244−2282 cm^{-1}. Theory predicts one strong b_{1u} harmonic at 2268.3 cm^{-1} and one strong b_{2u} harmonic at 2282.2 cm^{-1}. Actually these probably lie to the red of these positions, because the scaling factor of 0.958 does not fully account for the anharmonicity in these bands. The theoretical band intensities sum to about 1.8 times that of the experimental relative intensity, but as we mentioned earlier, we believe that theory overestimates the intensities of these bands by about a factor of 2, due primarily to limitations in the one-particle basis set. Thus, overall the agreement of the theoretical and experimental spectra is satisfactory, especially if account is taken of the fact that many more features appear in the experimental spectra due to matrix effects and the presence of overtone and combination bands.

Our matrix-isolation spectra of perdeuterated phenanthrene ($C_{14}D_{10}$) are given in Figures 2 and 4, and the "experimental"

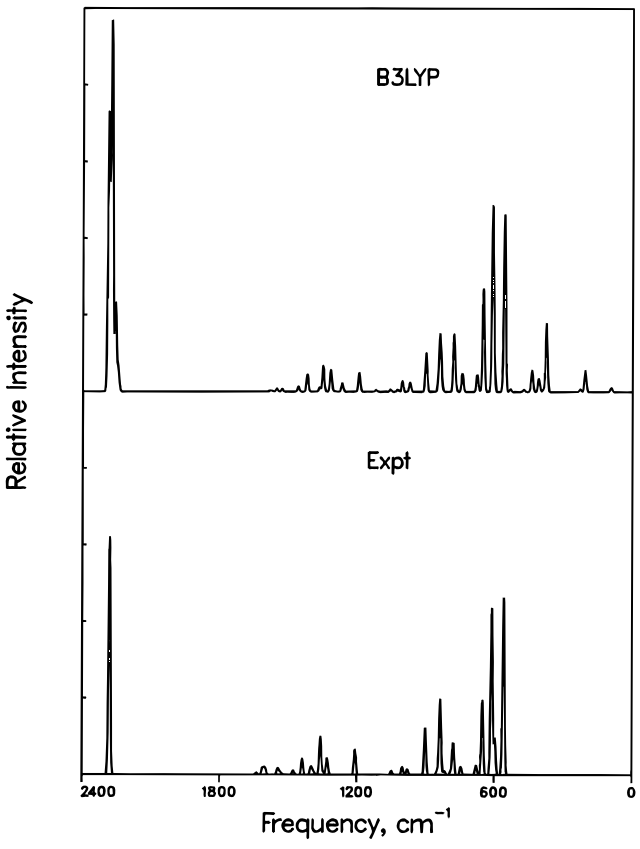

Figure 5. Comparison of synthetic phenanthrene-d_{10} spectra constructed using the experimental and theoretical data in Table 2. The fwhm is 10 cm^{-1}.

and theoretical spectra are compared in Figure 5. The infrared frequencies and intensities are compared in Table 2. It is clear from the table and Figure 5 that the agreement between the theoretical and experimental band positions and relative intensities is excellent. The strongest band observed experimentally is the C−D out-of-plane bend mode at 559.0 cm^{-1}, which is very near the strong b_1 scaled B3LYP harmonic at 558.8 cm^{-1}. Similarly the bands observed between 595 and 597 cm^{-1} and at 610.7 and 650.9 cm^{-1} are in almost perfect agreement with theory in both position and relative intensity. A number of moderately strong bands in the theoretical spectrum lie below 450 cm^{-1} and thus outside the spectral range of our instrument. As for naphthalene, their strength is correlated with the degree of C−D character in the bands as indicated by the isotopic ratio. The experimental bands at 677.8, 744.0, and 777.6 cm^{-1} also correlate well with the theoretical results, although the experimental relative intensities are slightly less. The weak experimental bands at 789.3 and 816.5 cm^{-1} do not correspond unambiguously to any scaled B3LYP harmonics and may be overtone/combination bands. Possibly the b_1 scaled B3LYP harmonic at 832.0 cm^{-1} correlates with the 816.5 cm^{-1} band, but more likely it is included along with the B3LYP harmonic at 838.9 cm^{-1} in the relatively strong and broad experimental band at 834.5 cm^{-1}. The experimental bands observed at 898.8 and 900.2 cm^{-1} correlate well with the theoretical a_1 harmonic at 899.8 cm^{-1}. As for naphthalene, the spectrum in the C−D in-plane bending and C−C stretch region between about 1000 and 1600 cm^{-1} is relatively weak. However, there is good correlation between the experimental and theoretical bands, except that additional weak bands are observed in the experimental spectrum that presumably correspond to overtone/combination bands, for example the band at 1638 cm^{-1}, which clearly does not correlate with any of the computed results.

Since the phenanthrene molecule does not have gerade/ungerade symmetry, all 10 C−D stretch harmonics are allowed and at least six carry appreciable intensity. The sum of the relative intensities for the theoretical bands is about 3.4 times

TABLE 2: Comparison of Theoretical and Experimental Infrared Frequencies (cm^{-1}) and Intensities (km/mol) for Perdeuterated Phenanthrene

	theory			experiment	
irrep	freq[a]	intensity[b]	ratio[c]	freq	rel int
b_1	92.7	0.58(0.024)	1.078		
b_1	205.5	2.97(0.121)	1.103		
a_1	227.8	0.36(0.015)	1.073		
b_1	375.6	9.53(0.387)	1.146		
a_1	389.0	0.34(0.014)	1.040		
b_2	408.9	1.81(0.074)	1.076		
b_1	439.2	2.99(0.121)	1.135		
b_2	473.4	0.29(0.012)	1.056		
a_1	532.6	0.36(0.015)	1.032		
b_1	558.8	24.61(1.000)	1.280	559.0	1.000
b_2	605.2	4.66(0.189)	1.037	595.4,596.9	0.205
b_1	611.0	23.94(0.973)	1.206	610.7	0.942
b_1	650.8	14.35(0.583)	1.256	650.9	0.422
a_1	664.5	0.09(0.004)	1.066	670.6	<0.01
b_2	677.6	2.33(0.095)	1.058	677.8	0.052
b_1	742.0	2.52(0.102)	1.174	744.0	0.045
a_1	772.2	0.77(0.031)	1.075	771	<0.01
b_2	776.4	0.12(0.005)	1.121		
b_1	778.5	7.64(0.310)	1.221	777.6	0.179
				789.3	0.018
				816.5	0.021
b_1	832.0	0.99(0.040)	1.188		
b_2	838.9	7.34(0.298)	1.191	834.5 broad	0.425
a_1	844.8	1.11(0.045)	1.226	841.4	<0.01
a_1	848.5	0.24(0.010)	1.288	848.1	0.023
b_2	849.2	0.08(0.003)	1.223		
a_1	899.8	5.39(0.219)	1.304	898.8,900.2	0.263
b_2	970.2	1.30(0.053)	1.218	977.6	0.030
a_1	1003.0	1.49(0.061)	1.199	998.2,1000.4	0.044
b_2	1024.4	0.27(0.011)	1.196		
b_2	1054.8	0.26(0.011)	1.221	1046.1,1047.2	0.021
a_1	1117.3	0.22(0.009)	1.119		
a_1	1192.3	2.61(0.106)	1.089	1205.3,1208.7	0.142
b_2	1267.0	1.14(0.046)	1.054	1261,1273,1284	<0.01
a_1	1300.7	0.09(0.004)	1.032	1290,1306	<0.01
b_2	1316.5	1.69(0.069)	1.079		
a_1	1318.0	1.37(0.056)	1.076	1325−1333	0.094
				1345.7	0.014
b_2	1350.4	3.60(0.146)	1.083	1356.9,1357.9,1360.9	0.216
a_1	1366.3	0.60(0.024)	1.057	1387.4	0.013
				1395.0	0.023
				1401.0	0.035
b_2	1419.9	2.36(0.096)	1.055	1435.9,1439.2	0.091
a_1	1458.9	0.71(0.029)	1.043	1476.1,1478.6	0.023
b_2	1529.9	0.35(0.014)	1.017	1530.5	0.013
				1540.4	0.018
a_1	1553.1	0.42(0.017)	1.027	1546.1	0.027
b_2	1574.1[d]	0.06(0.002)	1.019		
a_1	1581.0	0.15(0.006)	1.019	1598.1	0.024
				1603.7	0.028
				1612 complex	0.036
				1638.2	0.011
b_2	2241.0	0.24(0.010)	1.357		
a_1	2245.4	2.32(0.094)	1.356		
b_2	2245.8	0.73(0.030)	1.356		
b_2	2255.2	0.37(0.015)	1.355		
a_1	2257.3	11.96(0.486)	1.354		
a_1	2272.5	15.01(0.610)	1.348		
b_2	2272.7	22.78(0.926)	1.351	2311−2249[e]	1.343
a_1	2276.3	17.48(0.710)	1.351		
b_2	2286.1	25.80(1.048)	1.348		
a_1	2289.7	15.61(0.634)	1.351		

[a] The B3LYP/4-31G frequencies are scaled by 0.958. [b] The relative intensities are given in parentheses. [c] The ratio of the hydrogen/deuterium frequencies. [d] There is a small feature on a contaminant water band at 1573.6 cm^{-1} in the experimental spectrum that might correspond to this phenanthrene band. [e] The main bands are at 2274.2, 2278.6, and 2295.6 cm^{-1}. Other bands are at 2252.6, 2256.2, and 2309.1 cm^{-1}: see Figure 2.

experiment, which is a larger difference than for naphthalene. While the theoretical intensities are likely a factor of 2 too large, we believe that the matrix effects may cause a reduction in the intensity of C−D stretch for this system. The total intensities for C−D stretch for naphthalene and phenanthrene are 160.1 and 199.1 km/mol, respectively. Thus, the intensity per C−D bond is actually less for phenanthrene than naphthalene. This is possibly due to the fact that the C−D stretching motion is somewhat hindered in phenanthrene, due to the closer proximity of some of the deuteriums.

It is interesting to compare the out-of-plane bending modes in hydrogenated and perdeuterated phenanthrene. The frequency in cm^{-1}(relative intensity) of the four b_1 bands in the out-of-plane bending region are for phenanthrene-h_{10} 715.1(0.02), 736.7(1.00), 817.1(0.80), and 871.4(0.15). For phenanthrene-d_{10} they are 558.8(1.00), 611.0(0.97), 650.8(0.58), and 742.0-(0.10). If we make a one-to-one correspondence of these bands, then we produce the isotopic shifts given in Table 2 that lie between 1.17 and 1.28. If instead we make the correlation on the basis of relative intensity, namely, we make the identification 736.7:558.8, 817.1:611.0, 871.4:650.8, and 715.1:742.0, then the isotopic ratios are 1.318, 1.337, 1.339, and 0.964. Clearly these isotopic shifts are difficult to rationalize. An inspection of the normal coordinates shows that these bands are mostly C−H out-of-plane bends and that there is no one-to-one correspondence between the hydrogenated and perdeuterated systems. That is, the modes in the perdeuterated system are mixtures of those for the hydrogenated system, which also supports not using the intensity to make the correlation between these bands. The other neutral systems that we studied also show a significant reallocation of the intensity with perdeuteration, but do not yield an obvious one-to-one correspondence based on the intensities.

Our matrix-isolation spectra of perdeuterated pyrene ($C_{16}D_{10}$) are shown in Figures 2 and 6. The theoretical infrared frequencies and intensities for the infrared active ungerade modes of perdeuterated pyrene are compared with the experimental matrix data (this work) and the frequencies from earlier solution and solid data reported by Bree *et al.*[13] in Table 3. A comparison of the synthetic pyrene-d_{10} spectra (not shown) constructed using the experimental and theoretical data in Table 3 shows the same kind of agreement as for naphthalene (Figure 3) and phenanthrene (Figure 5). The frequencies under the column Bree *et al*. in Table 3 include both directly observed values and a complete set of harmonic frequencies determined for pyrene using an approximate force field derived from naphthalene data. The observed values followed by a question mark indicate that the assignment is uncertain. We have followed their assignment except for the band at 821 cm^{-1}, which we have reassigned from b_{1u} to b_{2u}. However, the average absolute error in the band positions is significantly reduced by switching the two lowest C−D stretching modes of b_{1u} and b_{2u} symmetry. For example, the average difference for the Bree *et al*. observed values and theory as given in Table 3 is 12.7 cm^{-1}, with a maximum error of 45.5 cm^{-1} (for the b_{2u} C−D stretch mode). With a redesignation of these bands, the average absolute error would be 9.8 cm^{-1}, with a maximum error of 30.1 cm^{-1} (for the b_{1u} C−D stretch mode). The average difference between the B3LYP frequencies and those calculated using the force field derived from naphthalene (the values denoted "calc" in Table 3) is 19.4 cm^{-1} with a maximum error of 58.2 cm^{-1} (for the b_{2u} C−C stretch mode). Thus, the approximate values for pyrene derived using force field data are sufficiently accurate to guide the assignment of experimental spectra.

As for phenanthrene, the experimental frequencies and relative intensities determined in the matrix-isolation experiments reported here agree very well with the theoretical values. For example, the experimental frequencies at 525.5, 567.7, and 604.0 cm^{-1} agree very well with the b_{2u} ring deformation mode at 531.4 cm^{-1} and the two b_{3u} out-of-plane C−D bending modes at 566.8 and 604.0 cm^{-1}. The two harmonics at 740.5 and 759.4 cm^{-1} must then correspond to the three complexes of bands centered at 727.1, 746.7, and 756.7 cm^{-1}. Matrix effects may be complicating the spectrum, since in the solid data only two peaks are observed at 745 and 755 cm^{-1}, in good agreement with theory. We believe that the weak peak observed in the matrix at 765.9 cm^{-1} and in the solid at 762 cm^{-1} may be a combination band (e.g. a combination of the two relatively intense b_{3u} bands observed in the solid at 202 and 568 cm^{-1}). The theoretical bands at 818.1 and 827.5 cm^{-1} correspond well to the experimental bands at 814.1 and at 831−833 cm^{-1}, except that theory places most of the intensity in the latter band and experiment in the former. Since these bands are of different symmetry, it is possible that the assignment should be reversed to bring the intensities into the best possible agreement. Theory correlates well with the experimental peaks at 841.3 and 948.3 cm^{-1}. The experimental band observed in the matrix at 1181.7 cm^{-1} and in the solid at 1188 cm^{-1} does not appear to correlate with any theoretical harmonic and is likely an overtone band of an out-of-plane bend. The b_{1u} and b_{2u} bands in the theoretical spectrum between 1285.4 and 1561.4 cm^{-1} correspond primarily to C−C stretch motions, as indicated by the relatively small isotopic ratios. These correlate fairly well with experiment although many additional weak bands are observed in the matrix. Finally, the sum of the relative C−D stretch intensities are almost a factor of 2 larger than the matrix data. As stated previously, we believe that this difference can be rationalized in terms of limitations in the present theoretical treatment. Thus,

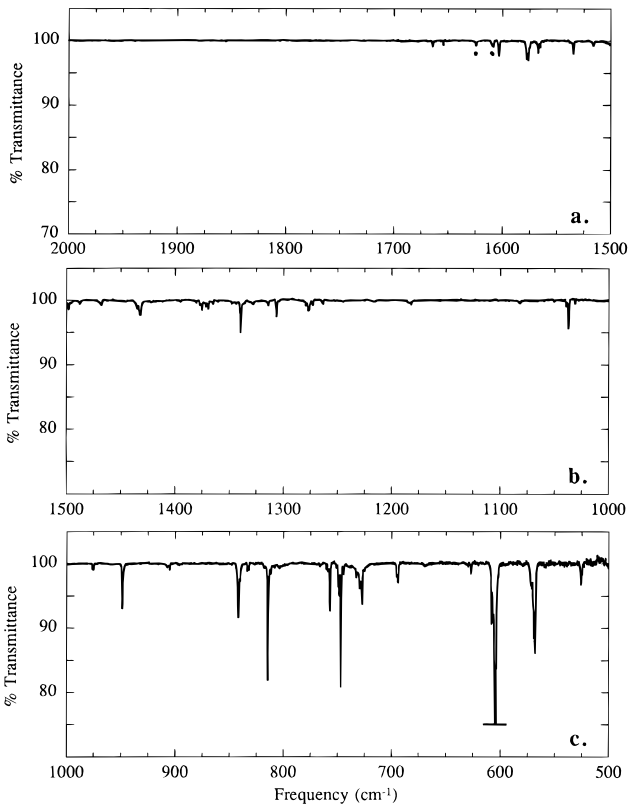

Figure 6. Spectra of matrix-isolated perdeuterated pyrene-d_{10} ($C_{16}D_{10}$) through the aromatic CC stretching and CD bending regions: (a) 2000−1500 cm^{-1}, (b) 1500−1000 cm^{-1}, and (c) 1000−500 cm^{-1}. The spectra were taken at 10 K, and the argon to pyrene-d_{10} ratio was in excess of 2000/1. Bands due to contaminant matrix-isolated H_2O are indicated with a dot (•).

TABLE 3: Comparison of Theoretical and Experimental Infrared Frequencies (cm^{-1}) and Intensities (km/mol) for Perdeuterated Pyrene

	theory, this work			experiment, this work		Bree *et al.*[13]	
irrep	freq[a]	intensity	ratio[b]	freq	rel int	calc[c]	obsd[d]
b_{3u}	92.1	0.40(0.009)	1.071			105	119
b_{3u}	192.3	7.43(0.175)	1.092			178	202
b_{2u}	328.4	1.23(0.029)	1.076			330	324
b_{3u}	436.8	0.67(0.016)	1.124			428	431
b_{1u}	464.9	2.17(0.051)	1.075			468	461
b_{2u}	531.4	2.18(0.051)	1.034	525.5	0.040	489	519
b_{3u}	566.8	15.92(0.374)	1.254	567.7	0.338	568	568
b_{3u}	604.0	42.53(1.000)	1.236	604.0	1.000	638	598
				626.6	0.019		
b_{1u}	670.0	0.01(0.000)	1.034	669	<0.01	626	
				693.9,695.2	0.041		
				727.1 complex	0.165		
b_{3u}	740.5	20.98(0.493)	1.146	746.7 complex	0.241	703	745
b_{1u}	759.4	2.63(0.062)	1.080	756.7 complex	0.086	711	755
				765.9	0.010		762
b_{2u}	818.1	3.37(0.079)	1.168	814.1	0.190	828	821?
b_{3u}	827.5	9.10(0.214)	1.180	831.7,833.0	0.020	798	804
b_{1u}	844.7	7.98(0.188)	1.180	841.3	0.185	814	841
b_{2u}	845.0	0.81(0.019)	1.374			833	
				896.0	0.013		
				904.4, 907.1	0.016		903
b_{2u}	948.1	4.10(0.096)	1.253	948.3	0.095	911	945
b_{1u}	967.4	0.78(0.018)	1.129	974.7,975.7	0.017	954	
b_{2u}	1035.1	1.74(0.041)	1.166	1036.7,1039.0	0.066	1016	1037
b_{1u}	1043.0	0.02(0.000)	1.202	1050.2	<0.01	1026	
				1181.7	0.019		1188?
				1263.1	0.011		
b_{2u}	1285.4	3.04(0.071)	1.023	1272.4,1276.2,1278.8	0.076	1271	1276
b_{1u}	1297.5	4.30(0.101)	1.100	1305.9	0.043	1314	
				1313.5	0.011		
b_{2u}	1323.8	2.24(0.053)	1.078	1327.7	0.010	1382	1338
				1339.2	0.085		
				1364.6−1380.1[e]	0.085		1366
b_{1u}	1401.4	3.15(0.074)	1.031			1392	1427
b_{2u}	1437.3	0.95(0.022)	1.027	1431.8 complex	0.107	1425	1461?
				1467.3	0.030		
				1497.7	0.033		
				1515.7	0.013		
				1534.0	0.030		
b_{1u}	1555.6	4.34(0.102)	1.020	1564.6,1566.5,1569.3	0.048	1588	1570?
b_{2u}	1561.4	0.54(0.013)	1.023	1575.6,1577.1	0.105	1564	1561
				1602.5	0.045		
				1663.5	0.011		
b_{1u}	2241.5	2.46(0.058)	1.357			2241	2256
b_{1u}	2246.5	0.24(0.006)	1.356			2247	2278
b_{2u}	2256.5	20.56(0.483)	1.353			2264	2211
b_{2u}	2272.1	49.10(1.154)	1.348	2245−2313[f]	1.510	2289	2242
b_{1u}	2278.5	53.50(1.258)	1.349			2292	2294

[a] Theoretical frequencies are multiplied by the factor of 0.958. [b] Calculated isotopic ratios: see ref 15 for frequencies for pyrene-h_{10}. [c] Calculated using the force constant from naphthalene. [d] The assignments are not certain if followed by a question mark; we have reassigned their 821 cm^{-1} band from b_{1u} to b_{2u}. Spectra were obtained for solids and in solution. [e] The main peaks are at 1368.9, 1374.7, and 1376.7 cm^{-1}: see Figure 6. [f] The main peaks are at 2263.2, 2269.8, 2273.3, 2284.3, 2287.8, and 2290.6. Others are at 2243, 2292.9, 2299.3, 2305.5, 2319, and 2322: see Figure 2.

overall the present B3LYP calculations are in good agreement with both the matrix isolation and solid state data.

In Table 4 we compare the theoretical frequencies for the gerade modes of pyrene and perdeuterated pyrene with those deduced from the Raman spectrum[13,26] and those calculated using an approximate force field. The relative agreement is comparable for both pyrene-h_{10} and pyrene-d_{10}. The average absolute differences between the scaled B3LYP results and those calculated with a force field are 20.8 and 20.3 cm^{-1} for pyrene-h_{10} and pyrene-d_{10}, respectively, whereas the analogous differences for the scaled B3LYP results and experiment are 11.6 and 12.1 cm^{-1}. Note that we have kept the assignments of Bree *et al*., although the 530 cm^{-1} band for pyrene-h_{10} would agree with theory better if it were reassigned from b_{2g} to b_{1g}. However, overall theory corroborates the experimental assignments of the Raman data and indicates that agreement is comparable for both the gerade and ungerade bands. We should also note that the low-frequency modes obtained in the solid that lie outside the spectral range of the spectrometer used in the matrix isolation work reported here also agrees very well with theory.

It is interesting to compare the out-of-plane bending fundamentals of hydrogenated and perdeuterated pyrene. For fully hydrogenated pyrene the three b_{3u} fundamentals have frequencies in cm^{-1} (relative intensities) of 710.9(0.27), 746.6(0.08), and 848.3(1.00). For perdeuterated pyrene the corresponding values are 566.8(0.37), 604.0(1.00), and 740.5(0.49). Thus, the total intensity is divided up into these three fundamentals very differently for the two cases. This is not an artifact of theory, because experiment supports the theoretical values.

Figures 2 and 7 show the matrix-isolation spectra of the largest system that we consider in this work, namely, perdeuterated chrysene ($C_{18}D_{12}$). The theoretical and experimental infrared frequencies and intensities are compared in Table 5.

TABLE 4: Comparison of Theoretical and Observed Raman Frequencies (cm^{-1}) for the *g*-Fundamentals of Pyrene

	pyrene-h_{10}			pyrene-d_{10}		
irrep	theory[a]	calc[b]	obsd[c]	theory[a]	calc[b]	obsd[c]
b_{1g}	246.5	251	263	221.4	224	235
b_{2g}	258.9	272	227	240.8	254	205
a_g	405.8	393	408	396.4	383	399
b_{3g}	455.6	425	458	434.4	411	437
b_{3g}	502.0	496	505	466.6	455	466
b_{2g}	504.2	469	530?	451.2	414	
b_{1g}	526.3	512		460.7	463	
a_g	577.0	607	593	552.9	579	564
b_{2g}	579.3	579		499.0	489	
b_{3g}	739.3	694	736	693.2	647	688[d]
b_{2g}	770.9	755	780?	614.2	600	618
a_g	803.3	737	805	751.9	703	752[d]
b_{1g}	803.9	811		646.5	653	
b_{2g}	826.9	764		759.6	754	770?
b_{1g}	908.7	899		764.4	739	
b_{2g}	966.2	947	971?	791.3	768	
b_{2g}	985.0	963		852.8	808	849?
a_g	1066.1	1058	1067	840.2	820	833
b_{3g}	1107.2	1077	1109	844.2	835	833[d]
a_g	1150.5	1142	1144	874.9	841	875
b_{3g}	1183.5	1160	1176	942.5	904	
a_g	1241.4	1232	1243	1156.3	1162	1164
b_{3g}	1250.8	1220		1044.3	1036	
a_g	1324.1	1300	1352	1260.0	1263	1275
b_{3g}	1361.7	1357	1373	1228.7	1198	1239
a_g	1389.6	1407	1408	1368.4	1358	1388
b_{3g}	1414.5	1383		1359.5	1313	1373?
b_{3g}	1498.0	1509		1421.3	1451	1433?
a_g	1552.0	1567	1552	1500.2	1517	1504
b_{3g}	1571.3	1601	1596	1555.5	1590	1582
a_g	1618.0	1656	1630	1595.7	1644	1619
b_{3g}	3041.8	3028	3015?	2241.9	2245	2252
a_g	3045.8	3021	3026	2246.0	2242	2273
b_{3g}	3054.2	3049	3049?	2257.0	2265	2273?
a_g	3063.4	3073	3059	2272.2	2287	2292
a_g	3074.4	3081	3102	2278.8	2294	2302

[a] Theoretical frequencies are multiplied by the factor of 0.958. [b] Calculated by Bree *et al.*[13] using the force constants from naphthalene. [c] Experimental work of Bree *et al.*: a question mark indicates that assignment is uncertain. The spectra were obtained for single crystals and in solution. [d] Value taken from fluorescence spectrum, ref 26.

As for the other systems considered in this work, there is overall good agreement, at least for the stronger bands. For chrysene there is more intensity in ring deformation modes than for the smaller systems. Note that our criterion for separating ring deformation from out-of-plane bending is whether the isotopic ratio is less than or greater than 1.10. Although this criterion is somewhat arbitrary, the split between ring deformations and out-of-plane bends in all the PAHs is probably meaningful. There is again a strong correlation between the strength of the bands and the degree of C−H(C−D) motion as indicated by the isotopic ratio.

The lowest frequency band observed in the matrix at 481.9 cm^{-1} agrees very well with our scaled B3LYP a_u harmonic at 480.1 cm^{-1}. The observed bands at 611.0, 624.7, and 649.9 cm^{-1} correspond well to the three a_u out-of-plane motions. Note that the isotopic ratio clearly identifies the b_u band at 647.6 cm^{-1} as due to ring deformation. It is unclear whether the band observed at 794.3 cm^{-1} corresponds to the b_u ring deformation mode at 790.8 cm^{-1} or to the a_u out-of-plane bending band at 797.8 cm^{-1}. Again, it is clear from the isotopic ratios that the bands between 994.4 and 1176.6 cm^{-1} in the theoretical spectra involve more in-plane bending motions than the bands at 1300.1 cm^{-1} and higher frequencies, which are primarily C−C stretch motions. Nevertheless, the intensity of these bands are significantly less for perdeuterated chrysene than hydrogenated chrysene. Finally, the sum of the relative intensities for the C−D stretch motions in chrysene is about a factor of 2.6 larger than observed in the matrix. Again, most of this difference can be attributed to an overestimation of these intensities in the calculations.

TABLE 5: Comparison of Theoretical and Experimental Infrared Frequencies (cm^{-1}) and Intensities (km/mol) for Perdeuterated Chrysene

	theory			experiment	
irrep	freq[a]	intensity[b]	ratio[c]	freq	rel int
a_u	45.8	0.11(0.002)	1.068		
a_u	71.5	0.19(0.003)	1.087		
b_u	173.4	0.43(0.008)	1.065		
a_u	210.3	4.34(0.079)	1.108		
a_u	267.5	0.27(0.005)	1.081		
a_u	375.6	11.56(0.211)	1.148		
b_u	445.5	8.18(0.149)	1.078		
a_u	480.1	9.12(0.166)	1.155	481.9	0.087
a_u	496.6	1.68(0.031)	1.167		
b_u	514.1	0.58(0.011)	1.047		
b_u	555.6	0.44(0.008)	1.027		
a_u	610.0	2.62(0.048)	1.201	611.0	0.021
a_u	623.6	54.82(1.000)	1.223	624.7	1.000
b_u	647.6	12.17(0.222)	1.058	644.8	0.186
a_u	650.9	14.33(0.261)	1.255	649.9	0.177
				674.9	0.089
a_u	764.5	4.57(0.083)	1.130	764.6	0.039
a_u	771.1	0.56(0.010)	1.228		
b_u	790.8	1.52(0.028)	1.074	794.3	0.028
a_u	797.8	2.20(0.040)	1.202		
b_u	801.3	0.39(0.007)	1.094		
a_u	841.0	1.24(0.023)	1.176	826.1	0.014
b_u	847.7	0.63(0.011)	1.217	844.6	0.027
b_u	852.5	2.25(0.041)	1.265		
b_u	868.6	9.65(0.176)	1.334	869.4,870.4	0.156
b_u	907.9	9.30(0.170)	1.290	909.6	0.072
b_u	994.4	3.12(0.057)	1.203	974.6 or 991.9	<0.01
				1033.8	0.015
b_u	1048.8	1.12(0.020)	1.182	1040.8	0.038
b_u	1112.2	0.70(0.013)	1.136	1103.3 or 1114.2	<0.01
b_u	1176.6	4.01(0.073)	1.108	1187.5,1189.7	0.099
b_u	1300.1	2.94(0.054)	1.036	1309.4	0.113
b_u	1327.1	1.75(0.032)	1.075	1333.7	0.014
b_u	1344.4	1.90(0.035)	1.067	1355.5,1356.9	0.023
b_u	1404.0	4.96(0.090)	1.058	1394.1,1396.2	0.024
				1420.1	0.162
b_u	1462.9	1.05(0.019)	1.035	1483.3	0.052
b_u	1553.4	1.87(0.034)	1.023	1539.9	0.011
b_u	1576.2	0.71(0.013)	1.019	1578.5	0.019
				1629.8	0.010
b_u	2245.5	0.65(0.012)	1.356		
b_u	2249.9	5.56(0.101)	1.355		
b_u	2257.5	20.97(0.383)	1.354		
b_u	2275.7	38.21(0.697)	1.351	2249−2322[d]	0.911
b_u	2286.6	19.89(0.363)	1.349		
b_u	2293.0	46.95(0.856)	1.353		

[a] The B3LYP/4-31G frequencies are scaled by 0.958. [b] The relative intensities are given in parentheses. [c] The ratio of the hydrogen/deuterium frequencies. [d] The main peak is at 2275.2 cm^{-1}: see Figure 2.

In Table 6 we compare the integrated intensities for the different vibrational motions of the hydrogenated and perdeuterated naphthalene, phenanthrene, pyrene, and chrysene neutral PAHs. Most of the intensity for all of these species is in the out-of-plane bends and C−H(C−D) stretches. The intensity of all of the modes is reduced for all of these species upon deuteration. For naphthalene, the sum of intensities is reduced from 336.3 to 188.6 km/mol upon deuteration, a reduction by a factor of 1.78. Except for the weak ring deformations, which are not strongly affected by the motion of the hydrogens (deuteriums), each of the modes is reduced by a comparable factor. For pyrene, deuteration reduces the overall intensities by a factor of about 1.75, and except for the weak ring deformation modes, this ratio holds rather well for all of the

TABLE 6: Comparison of Integrated Intensities (km/mol) for Fully Hydrogenated and Deuterated PAHs[a]

	naphthalene			phenanthrene			pyrene			chrysene		
mode	$C_{10}H_8$	$C_{10}D_8$	ratio	$C_{14}H_{10}$	$C_{14}D_{10}$	ratio	$C_{16}H_{10}$	$C_{16}D_{10}$	ratio	$C_{18}H_{12}$	$C_{18}D_{12}$	ratio
ring deformation	6.62	6.40	1.03	11.25	10.73	1.05	17.35	16.05	1.08	29.12	24.28	1.20
CH out-of-plane bend	131.64	71.47	1.84	164.97	89.44	1.84	166.60	92.57	1.80	195.04	103.18	1.89
CH in-plane bend and CC stretch	37.97	19.70	1.93	58.95	33.84	1.74	63.25	33.99	1.86	77.73	47.20	1.65
CH stretch	160.09	91.04	1.76	199.08	112.30	1.77	217.28	125.86	1.73	235.70	132.23	1.78
total	336.32	188.61	1.78	434.25	246.31	1.76	464.48	268.47	1.73	537.59	306.89	1.75

[a] Theoretical results for the deuterated species from this work and for the hydrogenated species from ref 15.

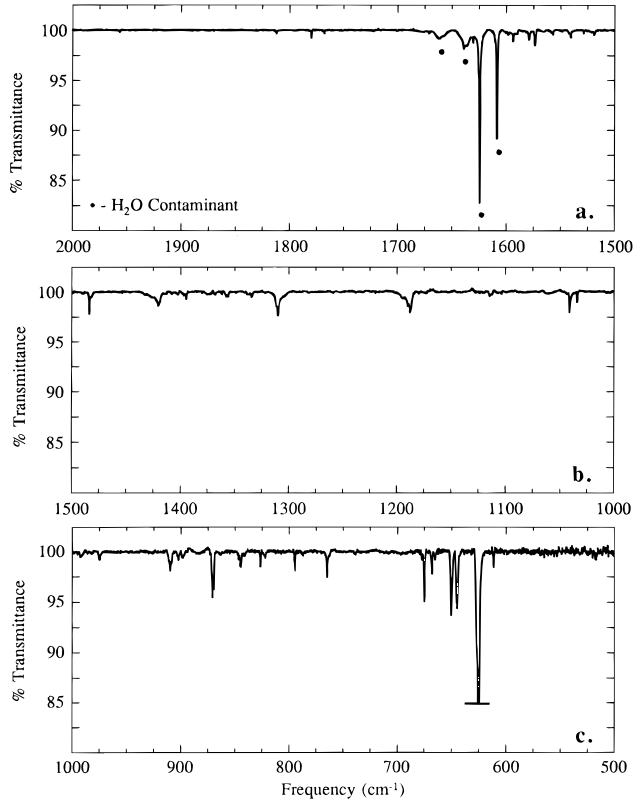

Figure 7. Spectra of matrix-isolated perdeuterated chrysene-d_{12} ($C_{18}D_{12}$) through the aromatic CC stretching and CD bending regions: (a) 2000−1500 cm^{-1}, (b) 1500−1000 cm^{-1}, and (c) 1000−500 cm^{-1}. The spectra were taken at 10 K, and the argon to chrysene-d_{12} ratio was in excess of 2000/1. Bands due to contaminant matrix-isolated H_2O are indicated with a dot (•).

motions, since all of the strong bands have significant C−H(C−D) involvement. Thus, the reduction in intensity upon deuteration is about the same for every PAH studied. The calculated magnitude of this reduction should be very accurate, as much of the error in the individual intensities cancel.

V. Conclusions

Density functional calculations and matrix-isolation experiments have been reported for perdeuterated naphthalene, phenanthrene, pyrene, and chrysene. The isotopic ratios are computed by combining these results with earlier analogous results for the fully hydrogenated species. The theoretical isotopic ratios are found to provide a good diagnostic for the type of vibrational motion associated with each band. The experimental and theoretical frequencies are in excellent agreement (average absolute error of less than 10 cm^{-1}). We find that perdeuteration reduces the overall intensities by about a factor of 1.75. This is true of all of the vibrational modes, except for the weak low-frequency ring deformation modes. Perdeuteration is also found to substantially reallocate the intensity in the various out-of-plane bending modes in some cases. The B3LYP calculations also support in most cases the assignments of the both the gerade and ungerade fundamentals of pyrene and perdeuterated pyrene determined from Raman and infrared spectra taken in solution and in the solid.

References and Notes

(1) Allamandola, L. J.; Tielens, A. G. G. M.; Barker, J. R. *Astrophys. J. Suppl. Ser.* **1989**, *71*, 733.
(2) Puget, J. L.; Leger, A. *Annu. Rev. Astron. Astrophys.* **1989**, *27*, 161.
(3) Allamandola, L. J.; Sandford, S. A.; Wopenka, B. *Science* **1987**, *237*, 56.
(4) Tielens, A. G. G. M.; Allamandola, L. J.; Barker, J. R.; Cohen, M. In *Polycyclic Aromatic Hydrocarbons and Astrophysics*; Leger, A., d'Hendecourt, L. B., Eds.; D. Reidel Publishing Co.: Dordrecht, 1986; pp 255−271.
(5) Kovalenko, L. J.; Maechling, C. R.; Clemett, S. J.; Philippoz, J. M.; Zare, R. N.; Alexander, C. M. O'D. *Anal. Chem.* **1992**, *64*, 682.
(6) Clemett, S.; Maechling, C.; Zare, R.; Swan, P.; Walker, R. *Science* **1993**, *262*, 721.
(7) Robert, F.; Javoy, M.; Halbout, J.; Dimon, B.; Merlivat, L. *Geochim. Cosmochim. Acta* **1987**, *51*, 1787.
(8) McKeegan, K. D.; Walker, R. M.; Zinner, E. *Geochim. Cosmochim. Acta* **1985**, *49*, 1971.
(9) Geiss, J.; Reeves, H. *Astron. Astrophys.* **1981**, *93*, 189.
(10) Kerridge, J. F.; Chang, S.; Shipp, R. *Geochim. Cosmochim. Acta* **1987**, *51*, 2527.
(11) Yang, J.; Epstein, S. *Geochim. Cosmochim. Acta* **1983**, *47*, 2199.
(12) Robert, F.; Epstein, S. *Geochim. Cosmochim. Acta* **1982**, *46*, 81.
(13) Bree, A.; Kydd, R. A.; Misra, T. N.; Vilkos, V. V. B. *Spectrochim. Acta* **1971**, *27A*, 2315.
(14) Califano, S.; Abbondanza, G. *J. Chem. Phys.* **1963**, *39*, 1016.
(15) Langhoff, S. R. *J. Phys. Chem.* **1996**, *100*, 2819.
(16) Stephens, P. J.; Devlin, F. J.; Chablowski, C. F.; Frisch, M. J. *J. Phys. Chem.* **1994**, *98*, 11623.
(17) Becke, A. D. *Phys. Rev. A* **1988**, *38*, 3098.
(18) Lee, C.; Yang, W.; Parr, R. G. *Phys. Rev. B* **1988**, *37*, 785.
(19) *Gaussian 92/DFT*, Revision G.2; Frisch, M. J., Trucks, G. W., Schlegel, H. B., Gill, P. M. W., Johnson, B. G., Wong, M. W., Foresman, J. B., Robb, M. A., Head-Gordon, M., Replogle, E. S., Gomperts, R., Andres, J. L., Raghavachari, K., Binkley, J. S., Gonzalez, C., Martin, R. L., Fox, D. J., Defrees, D. J., Baker, J., Stewart, J. J. P., Pople, J. A. Gaussian, Inc.: Pittsburgh, PA, 1993.
(20) Frisch, M. J.; Pople, J. A.; Binkley, J. S. *J. Chem. Phys.* **1984**, *80*, 3265, and references therein.
(21) Bauschlicher, C. W.; Langhoff, S. R. *Spectrochim. Acta*, in press.
(22) Joblin, C.; d'Hendecourt, L.; Léger, A.; Défourneau, D. *Astron. Astrophys.* **1994**, *281*, 923.
(23) Hudgins, D. M.; Allamandola, L. J. *J. Phys. Chem.* **1995**, *99*, 3033.
(24) Hudgins, D. M.; Sandford, S. A.; Allamandola, L. J. *J. Phys. Chem.* **1994**, *98*, 4243.
(25) Zhang, K.; Guo, B.; Colarusso, P.; Bernath, P. F. *Science* **1996**, *274*, 582.
(26) Bree, A.; Vilkos, V. V. B. *Spectrochim. Acta* **1971**, *27A*, 2333.